



Published in final edited form as:

J Thorac Cardiovasc Surg. 2019 March ; 157(3): 932–940.e3. doi:10.1016/j.jtcvs.2018.07.103.

PERFORMANCE AND HEALING OF AN EXPANDED POLYTETRAFLUOROETHYLENE MULTI CHORDAL DEVICE AT 6- MONTHS AFTER REPAIR OF MITRAL LEAFLET FLAIL IN SWINE

Surendra K. Chawla, MD¹, Robert W.M. Frater, MD², Mark Cunningham, PhD³, Muralidhar Padala, PhD⁴

^[1]Division of Cardiothoracic Surgery, St. Francis Hospital and Medical Center, Hartford, CT, USA;

^[2]Robert W. M. Frater Center for Cardiovascular Research, University of Free State, Bloemfontein, South Africa;

^[3]SURPASS, Osceola, WI;

^[4]Structural Heart Research and Innovation Laboratory, Division of Cardiothoracic Surgery, Emory University School of Medicine, 10 Atlanta, GA, USA

STRUCTURED ABSTRACT:

Objective: Repairing a prolapsing mitral valve that involves multiple cusps, is procedurally complicated and carries a higher risk of failure when performed with individual neochordae. Inserting multiple neochordae into the papillary muscle, sizing and aligning them in a manner that can restore coaptation is challenging. A multi-chordal mitral valve apparatus (MitraPatch) with a single neo-papillary muscle section, four neochordae with each chord ending in a neoleaflet section was developed. In this study, the 6-month outcomes of using this apparatus to repair mitral prolapse in swine is reported.

Methods: Seven pigs (n=7) with prolapse from mitral chordal transection were repaired with the device. 1 pig was acutely terminated to develop the procedure, and 6 swine were survived to 150 days (n=4) and 180 days (n=2), with monthly echocardiographic examinations. At termination, all hearts were explanted for gross necropsy and detailed histopathology.

Results: Severe mitral regurgitation was created after chordal transection in all the pigs. Repairing the valve with the device reduced MR to none-or-trace levels in 3 swine, grade 1 MR in 3 swine and 1–2+ in 1 swine immediately after surgery. In the pigs with none/trace/grade 1 MR, the device was intact and coaptation was fully restored as observed on serial echocardiograms. The device was intact, without dehiscence, stretching or fibrosis at termination. The neo-leaflet and neo-papillary sections of the device elicited a host response, which we know is on track to product

Corresponding author: Muralidhar Padala PhD, 380-B Northyards Blvd, Atlanta, GA 30313, United States of America, spadala@emory.edu, 404-251-0651 (Phone), 404-251-0660 (Fax).

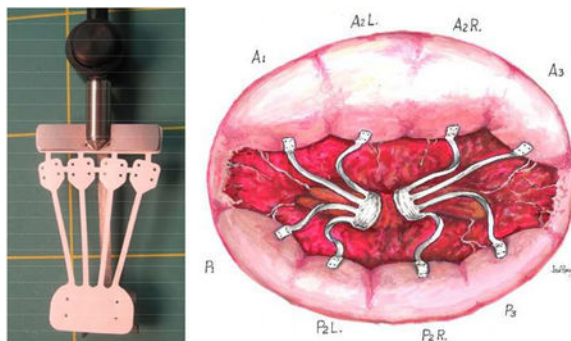
Publisher's Disclaimer: This is a PDF file of an unedited manuscript that has been accepted for publication. As a service to our customers we are providing this early version of the manuscript. The manuscript will undergo copyediting, typesetting, and review of the resulting proof before it is published in its final citable form. Please note that during the production process errors may be discovered which could affect the content, and all legal disclaimers that apply to the journal pertain.

Conflict of Interest: SKC discloses assignment of a patent application on this design. RWMF, MC, and MP do not have any conflicts of interest to disclose.

living valve replacement tissue, but we cannot tell how controlled this might be several years later. In the pig with grade 1–2+ MR accidental transection of both marginal and strut chordae in that region was observed at termination, with dehiscence of the device at the site of its insertion into the leaflet.

Conclusion: The anatomical principles that guide this multi-chordal design appear to be valid, with good hemodynamic performance and a controlled host response at 6 months.

CENTRAL PICTURE



Central picture legend: A device with a papillary muscle section, multiple chordae with neoleaflets for mitral repair.

CENTRAL MESSAGE: The multi-chordal mitral repair device, has a theoretical benefit in performing complex mitral repairs. This study reports the 6-month feasibility and performance of this device in swine.

PERSPECTIVE STATEMENT: A general tendency exists to choose mitral valve replacement over mitral valve repair, in lesions that are complex from involvement of multiple cusps. A device design that can simplify repair, despite lesion complexity, can encourage surgeons without concentrated mitral repair experience to adopt repair into their everyday practice.

INTRODUCTION:

As experience with surgical repair of degenerative MV lesions increases with time, repairs involving multiple cusps and leaflets are being attempted. Such repairs are complicated, as combining leaflet resection and re-suspension with multiple neochordae to both PMs are necessary. When the AL is involved, challenges with limited tissue and properly sizing the neochordae, causes non-uniform leaflet coaptation and remnant MR. Experienced mitral surgeons seem to succeed at these complicated techniques, but the average surgeon often struggles. Inability to adequately restore valve competence leads to chordal sparing valve replacement to avoid a sub-optimal result after prolonged cardiac arrest time. A need exists to simplify repairs for excessively diseased valves, especially involving the AL.

Earliest techniques for repair of such valves, included posterior leaflet plication¹, limited resection², modified resection³, and quadrangular resection⁴. Though applicable for PL repair, lack of tissue restricts their application to the AL. Other non-resective techniques emerged subsequently, which included strut chordal transfer^{5–78} and leaflet flip over⁹¹⁰,

which had good clinical outcomes but did not gain widespread use due to the perceived risk of converting a one leaflet lesion into a bileaflet one. Use of ePTFE chordae as chordal substitutes was experimented by Frater RWM¹¹ and Revuelta¹², and clinically adopted by David et al¹³. Durability of ePTFE chordae has led to their extensive use, and neochordoplasty is now a technique of choice. Despite its success, proper sizing of neochordae remains a challenge as the procedure is performed on a flaccid heart, but its accuracy cannot be assessed until the heart is beating, and the slippery nature of ePTFE that complicates knot typing. Different techniques, tools^{14–23} and algorithms²⁴ to determine optimal size were reported, and configurations such as pre-measured chordae are now in use^{25, 26}. Borger et al. summarized the limitations and challenges with all of these techniques, concluding that anatomical dimensions in a fully loaded state may be the best guides²⁷.

An anatomical rule inherent to the mitral valve is that the distance between the papillary muscle base and leaflet insertions of the chordae emanating from it are equal. We sought to build upon this anatomical rule, by designing a synthetic patch, with a leaflet section, multiple chordae that end in a PM attachment (MitraPatch), for repair of extensive MV disease. In an earlier study, we reported the feasibility of MV repair with this patch in *in vitro* disease models²⁸, and developed a staged technique to effectively implant the device²⁹. Here we report our 6-month experience (162±15.2d post-implant) in swine induced with MVP.

MATERIALS AND METHODS:

“MitraPatch” implant design:

The implant was laser cut from a 25.4 mm long, 0.076mm thick, ePTFE tube, in a circumferential direction to achieve a tensile strength of 3 to 4 lbf, resulting in the design shown in Figure 1A. The implant has an expanded neo-PM (15mm × 8mm), four neochordae (18mm × 1mm) emerging from the same PM section, and each chord with a neoleaflet (5mm × 5mm); with the entire implant mounted onto a delivery handle. The assembly was ethylene oxide sterilized and sterile packaged.

Animal care and mitral valve surgery:

Studies were performed at an AAALAC accredited laboratory, with IACUC approval. Seven female Landrace cross-bred swine (3.7–4.7 months old, 54.3 – 60.6 kg) were purchased from Oak Hill Genetics, and used in this study. Animal handling and care protocols are described in the online supplement. Under anesthesia, and via a left thoracotomy, the pigs were placed on cardiopulmonary bypass support and the mitral valve was exposed via a left atriotomy. A2 flail was induced by marginal chordal transection. In the first pilot animal, transapical beating heart chordal transection with echocardiography was used, but control over the flail severity was lacking. In the next six animals, chordae were transected while on pump. A left thoracotomy was performed between the 4th- 5th intercostal space to access the heart, and cannulation was achieved in the descending aorta (arterial) and right atrial appendage (venous). Cardiac arrest was achieved with cold crystalloid Plegisol(Hospira,Inc), the aorta was cross clamped, and the mitral valve was accessed via the left atrium. A saline

test was performed to confirm valve closure, and repeated after the marginal chordae inserting into the AL were transected to create MR. Two 5"0" monofilament stay sutures were placed on either sides of the flail segment, to mark the native "reference chordae" surrounding the ruptured chordae. The device was inserted through the MV, and the neo-PM was sutured to the native PM at its base with two 5-0 ePTFE pledgeted sutures. The neochordae length was confirmed by aligning the native chordo-leaflet junction with the device chordo-leaflet junction. A pledgeted 6-0 ePTFE suture was used with a ventricular pledget (native pericardial pledget in 3 animals and ePTFE pledget in others) for leaflet attachment of the device. We described the physiological basis for this technique earlier, so it eliminates the need for frequent chordal sizing²⁴. Saline test was repeated and reduction in MR was recorded. The left atriotomy was closed, heart was reanimated, and decannulated. A chest tube was used, and the thoracotomy was closed in layers with skin closure using subcuticular suture. Furosemide was administered for diuresis and additional analgesia. Details of further post-operative care are described in the online supplement.

Echocardiography:

Transthoracic echo was performed under sedation at pre-and post-surgery, at weeks 1, 4, 8, 13, 22 and 26 after surgery. MR severity, peak and mean MV gradients, presence of remnant MVP, implant integrity, stability and mineralization were assessed.

Necropsy and tissue collection:

Necropsy was planned between 150–180 days (i.e. 5–6 months) after the surgery, and the specific necropsy times for each animal are indicated in Table 2. After heparinizing with 250–350 U/kg heparin (IV) and termination with an overdose of intravenous pentobarbital, the heart was extracted for necropsy. The heart was dissected carefully, and the device was photographed through the left atrium. The right atrium, the aortic valve and the tricuspid valve were removed, and the remaining heart was immersed in neutral buffered formalin for histopathology.

Histopathology:

Prior to sectioning, the base of the heart was removed to photograph the superior aspect of the MV. A digital radiograph was acquired to assess calcification, a portion of the leaflet and PM attachment were dissected for scanning electron microscopy, and the remainder was submitted for plastic processing and sectioning. For electron microscopy, the *en face* sections were rinsed in 0.1M sodium phosphate buffer, post fixed in a 1% osmium tetroxide solution for 30 minutes, dehydrated in a graded series of ethanol concentrations, and after critical point drying the tissue was sputter coated with gold. Specimens were visualized under a Hitachi S-3400 and S-3600 electron microscope. Histological sections were dehydrated in a graded series of ethanol and embedded in methyl methacrylate plastic. After polymerization, the device was sectioned with the leaflet and PM attachment in the longitudinal plane, and the neochordae in the transverse plane with an Ektat linear grinding machine. Final slides were polished and stained with toluidine blue and basic fuchsin stains. All sections were examined under light microscopy to assess host response and healing, thrombosis, inflammation, and injury. Hematoxylin and eosin staining was performed on the

AL and movat's pentachrome staining was performed on the PL cusps opposite to the device insertion site, to assess for unintended damage from the device.

Data analysis and statistical considerations:

Data is expressed as mean \pm standard deviation, and statistical analysis was performed in MS Excel. Qualitative observations were performed by an expert pathologist (CV Path Institute, Maryland) who did not have any conflict with this study.

RESULTS

Surgical success and functional outcomes:

Table 1 summarizes the study outcomes. The first pig (15P098) was terminated acutely as planned and the remaining six pigs (15P050, 15P099, 15P100, 15P101, 15P103, 15P104) were survived after surgery. A2 flail was evident in all the pigs, with severe MR recorded on the saline test. In pig 15P050, basal and strut chordae were accidentally transected in addition to the marginal chord to the A2 free edge. In the remaining animals, the marginal chordae to A1-A2 were transected. In the chronic surviving pigs, the flail could be repaired with one neochord in four animals, and with two neochordae in two animals. The unused neochordae on the device were cut and removed. The chronic animals survived the entire duration of the intended follow-up without issues. Terminal necropsy demonstrated an intact device and no leaflet flail in the one acute animal (Figure S2A) and five out of six chronic animals (Figure 2A–B and Figure S2B). In the pig 15P050 in which 2–3+ MR was observed within 6 days after implantation and which persisted for rest of the study duration, necropsy at 180 days demonstrated that a strut chord was transected in error at the time of surgery (Figure 2C). The device dehisced at its leaflet attachment, while its PM attachment and the neochorda was still intact. No such issues were seen in the remaining animals.

Echocardiographic observations:

Individual animal echocardiography observations and measurements are listed in Table 2. Severe MR was observed in all the animals prior to the repair by saline testing. Immediately after repair, MR grade of none or trace in three animals, grade 1 in three animals and 1–2 in one animal, were noted. Except for the animal 15P050 where an additional strut chord was accidentally cut, in the remaining five animals there was no MR progression (none to trace in 3 animals and 1+ in 2 animals). The transvalvular gradient ranged from 0.8 mmHg to 1.3 mmHg (mean of 1.04 mmHg), cardiac output from 3.1 to 6.7 lpm (mean of 4.9lpm), ejection fraction from 52 to 66%, absent MVP or flail of AL and PL, with the device intact and stable, indicating successful repair. Recurrence of severe MR was not evident, MR gradients were within physiological levels, and other physiological parameters and gross observations of the device were not abnormal (Table S2).

Explant radiography and histopathology:

A representative radiographic image from pig 15P103 is shown in Figure 3A, depicting the PM, device, and the native leaflet at necropsy. Calcific deposits were minimal, except in one animal in which a small opaque nodule was observed in the leaflet pledget (pig 15P103), which on histopathology was described as metaplastic ossification of the pledget (Figure

3B). At termination, adequate healing around the leaflet and PM attachment zones were observed (Figure 4A–B), characterized by endocardial tissue formation that encapsulated the device and the pledget. Beneath the pledget at the PM insertion site, well demarcated regions of granulation tissue with multinucleated giant cells were observed. The healing response to pericardial and PTFE pledget was similar, without any striking differences evident on histopathology. Endothelialization of the leaflet and PM attachment sites was observed (Figure 5A–B), but not on the chordal aspect of the device. In all the explants, the neochordae isolated from the leaflet and PM sections, did not demonstrate abnormal stretching, degeneration, mineralization or fibrous pannus formation. In two animals 15P099 and 15P101 there was an organized thrombus near the atrial attachment site with no evidence of embolization. The posterior leaflet section opposite to the device demonstrated slightly granular darkened tissue but not endothelial denudation, tissue tearing, damage or severe inflammatory response (Figure 5C–D). The host response to the device seemed to be on track to develop living replacement tissue, but we cannot predict how controlled this could be after several years.

DISCUSSION

Key study findings:

This data demonstrates the 6-month feasibility and proof-of-concept of the device for mitral repair, supporting further development. The ePTFE thickness, dimensions of the neopapillary muscle, chordae and neoleaflet section were adequate to resist device stretching. 30 μ material porosity was optimal for tissue ingrowth without blood cell aggregation or thrombosis(13). Procedurally, the single PM attachment simplified the task, and reduced injury. Dehiscence of the device at the papillary muscle was absent in all the animals. Availability of the four chordae enables repair of a large mitral leaflet segment, with the provision to cut and remove them if not used. By attaching the device to either the anterior or posterior PM, the four scallops served by chordae from each PM can be adequately repaired. Thus, with two such devices (central picture), chordal support to the entire valve can be restored. Furthermore, the expanded neoleaflet sections simplify their attachment, reducing the risk of dehiscence by distributing the load over the entire attachment surface. This mimics the native chordal insertion mechanics described previously by Padala³⁰ and Fenoglio³¹. Dehiscence of the device at the leaflet insertion site was observed in 1 animal, with the dehiscence occurring between 150–180 days post implantation. Upon termination and examination of the valve, erroneous transection of a major secondary strut chordae along with the marginal chord was observed, and a relatively large segment of the leaflet was supported by a single neochordae from the device. Radiography of the explanted valves did not show any calcific nodules on the ePTFE sections, but an opaque nodule (metaplastic ossification) was observed on the pericardial pledget in one valve. Thrombogenicity was also minimal, with no evidence of systemic embolization to the major organs. Healed thrombi were observed near the regions of the leaflet attachment in two animals, possibly related to blood seepage between the leaflet and the pledget used to reinforce the device attachment to the leaflet. Though only Aspirin and Plavix were used post-operatively in this study, short term anticoagulation with Warfarin may inhibit these small thrombi until endothelialization of these surfaces is achieved.

Endothelialization of the device at the attachment sites was evident on scanning electron microscopy, but such endothelial lining did not seem to extend into the neochordae. Lack of endothelium in these regions did have any adverse effects on the device function or increase the risk of thrombosis.

Rationale for device design & potential clinical applications:

Anatomically the length of the chordae tendineae are equal from their leaflet insertions to the base of the PM, while they vary in relation to the tip of the PM in human hearts³² (Figure 1B–C). In the developing fetal human heart, the two PMs originate from a planar myocardial bridge formed from the trabeculae, which spans from the anterior to the posterior myocardium, through the ventricular apex (Figure 1D). This myocardial bridge terminates in the atrioventricular cushions on either end. As the ventricle grows in size, the base of the papillary muscles move away from the annular plane, and the cushion tissue and the muscles themselves start to stretch in between. The resulting stretch pattern, sculpts the chordae tendineae and the individual leaflet heights, but the overall distance from the leaflet insertions to the base of the papillary muscle are preserved. Thus, attaching the device to the base of the papillary muscle eliminates the need for chordal sizing. This device design may aid in the repair of distinct MV pathologies. A single device could allow repair of small flail segments, or large prolapsing cusps. MR due to a damaged leaflet from extensive healed endocarditis can be repaired, by excising the damaged portion and replacing the defect with pericardial or synthetic material, and chordal support with this device. Such a repair is perceivable even for reconstructing a mitral leaflet affected by rheumatic heart disease. Ischemic mitral regurgitation secondary to restricted P3 segment can be repaired by transecting the restrained chordae to create flail, and then repaired with this device.

Limitations:

As with any experimental study, some limitations must be considered. The study was conducted over 6-months, which is sufficiently chronic, but is limited in relation to the human scenario. The potential benefit of adding an annuloplasty ring was not considered, and neither was the device compared against neochordae in the same model. This study was also limited to a single mitral valve pathology, and further studies are warranted in different lesions.

CONCLUSION

The anatomical principles that we have adopted in the design of this device and development of procedural steps, appear to be valid. Valve function and host-response to the device are on track in this six month study, but longer term device performance and healing cannot be deduced.

Supplementary Material

Refer to Web version on PubMed Central for supplementary material.

ACKNOWLEDGEMENTS

The authors acknowledge Mr. Dale Groth for his assistance with the surgeries.

Sources of Funding: Dr. Padala was supported by grant awards NIH 1R01HL135145-01A1, 1R01HL133667-01A1, 1R01HL140325-01A1, and American Heart Association grant 14SDG20380081 when writing and editing this manuscript.

ABBREVIATIONS

MV	mitral valve
e-PTFE	expanded polytetrafluoroethylene
MR	mitral regurgitation
PMPM	postero-medial papillary muscle
ALPM	antero-lateral papillary muscle
AL	anterior leaflet
PL	posterior leaflet
MVP	mitral valve prolapse

REFERENCES

1. McGoon DC. Repair of mitral insufficiency due to ruptured chordae tendineae. *Journal of Thoracic and Cardiovascular Surgery*. 1960;491-8.
2. Manhas DR, Hessel EA, Winterscheid LC, Dillard DH and Merendino KA. Repair of mitral incompetence secondary to ruptured chordae tendineae. *Circulation*. 1971;43:688-97. [PubMed: 4931291]
3. Yacoub M, Halim M, Radley-Smith R, McKay R, Nijveld A and Towers M. Surgical treatment of mitral regurgitation caused by floppy valves: repair versus replacement. *Circulation*. 1981;64:II210-6. [PubMed: 7249325]
4. Carpentier A, Relland J, Deloche A, Fabiani JN, D'Allaines C, Blondeau P, Piwnica A, Chauvaud S and Dubost C. Conservative management of the prolapsed mitral valve. *The Annals of thoracic surgery*. 1978;26:294-302. [PubMed: 380485]
5. Carpentier A Cardiac valve surgery--the "French correction". *The Journal of thoracic and cardiovascular surgery*. 1983;86:323-37. [PubMed: 6887954]
6. Lessana A, Escorsin M, Romano M, Ades F, Vergoni W, Lorenzoni D, Menozzi C and Monducci I. Transposition of posterior leaflet for treatment of ruptured main chordae of the anterior mitral leaflet. *The Journal of thoracic and cardiovascular surgery*. 1985;89:804-6. [PubMed: 3990333]
7. Obadia JF, Casali C, Chassignolle JF and Janier M. Mitral subvalvular apparatus: different functions of primary and secondary chordae. *Circulation*. 1997;96:3124-8. [PubMed: 9386184]
8. Padala M, Cardinau B, Gyoneva LI, Thourani VH and Yoganathan AP. Comparison of artificial neochordae and native chordal transfer in the repair of a flail posterior mitral leaflet: an experimental study. *Ann Thorac Surg*. 2013;95:629-33. [PubMed: 23291143]
9. Duran CG. Repair of anterior mitral leaflet chordal rupture or elongation (the flip-over technique). *Journal of cardiac surgery*. 1986;1:161-6. [PubMed: 2979918]
10. Chawla SK, Missri J, Wessel R. Mitral Valve repair for mitral regurgitation utilizing intraoperative transesophageal echocardiography-late results. *Connecticut Medicine*. 1996;8:455-460.

11. Vetter HO, Burack JH, Factor SM, Mancluso F and Frater RWM. Replacement of chordae tendineae using new expanded ptfе suture in sheep In: Bodnar E and Yacoub M, eds. Biologic and Bioprosthetic Heart Valves New York: New York Medical Books; 1986.
12. Revuelta JM, Garcia-Rinaldi R, Gaitе L, Val F and Garijo F. Generation of chordae tendineae with polytetrafluoroethylene stents. Results of mitral valve chordal replacement in sheep. *J Thorac Cardiovasc Surg.* 1989;97:98–103. [PubMed: 2642992]
13. David TE, Bos J and Rakowski H. Mitral valve repair by replacement of chordae tendineae with polytetrafluoroethylene sutures. *J Thorac Cardiovasc Surg.* 1991;101:495–501. [PubMed: 1999944]
14. Joshi P, Shukla R, Shi WY and Smith JA. Manual Braiding of GoreTex Neochords to Ensure Correct Length in Mitral Valve Repair. *Heart, lung & circulation.* 2017.
15. Prinzing A, Bleiziffer S, Krane M and Lange R. Initial Experience With a New Mitral Ring Designed to Simplify Length Determination of Neochords. *Ann Thorac Surg.* 2018.
16. Rodriguez-Roda J, Migueleña J, Lopez J, Martin M and Munoz R. How to Adjust Neochordae Length Accurately in Degenerative Mitral Regurgitation. *Ann Thorac Surg.* 2018;105:e183–e184. [PubMed: 29247615]
17. Mahfouz RA. Utility of the posterior to anterior mitral valve leaflets length ratio in prediction of outcome of percutaneous balloon mitral valvuloplasty. *Echocardiography.* 2011;28:1068–73. [PubMed: 21966895]
18. Moorjani N, Viola N, Janusauskas V and Livesey S. Adjusting the length 319 of artificial polytetrafluoroethylene chordae in mitral valve repair by a single loop technique. *J Thorac Cardiovasc Surg.* 2009;138:1441–2. [PubMed: 19660314]
19. Fattouch K, Bianco G, Sbraga F, Sampognaro R and Ruvalo G. Simple, safe and easy technique to ensure the correct length of artificial chordae in mitral valve repair. *Ann Thorac Surg.* 2007;83:1902–3. [PubMed: 17462435]
20. Cimen S, Ketenci B, Ozay B and Demirtas M. Neo-chordae length adjustment in mitral valve repair. *European journal of cardio-thoracic surgery : official journal of the European Association for Cardio-thoracic Surgery.* 2006;29:843–4. [PubMed: 16520045]
21. Matsui Y, Fukada Y, Naito Y, Sasaki S and Yasuda K. A new device for ensuring the correct length of artificial chordae in mitral valvuloplasty. *Ann Thorac Surg.* 2005;79:1064–5. [PubMed: 15734448]
22. Duran CM and Pekar F. Techniques for ensuring the correct length of new mitral chords. *The Journal of heart valve disease.* 2003;12:156–61. [PubMed: 12701786]
23. Sarsam MA. Simplified technique for determining the length of artificial chordae in mitral valve repair. *Ann Thorac Surg.* 2002;73:1659–60. [PubMed: 12022582]
24. Padala M The arithmetic of a successful mitral valve repair. *J Thorac Cardiovasc Surg.* 2017;154:1638–1640. [PubMed: 28888372]
25. Gillinov M, Quinn R, Kerendi F, Gaudiani V, Shemin R, Barnhart G, Raines E, Gerdisch MW and Banbury M. Premeasured Chordal Loops for Mitral Valve Repair. *Ann Thorac Surg.* 2016;102:e269–e271. [PubMed: 27549563]
26. Ghavidel AA, Samiei N, Javadikasgari H and Bashirpour K. Premeasured neochordae loop maker: a new technology in mitral valve repair. *Innovations (Phila).* 2013;8:443–9. [PubMed: 24356435]
27. Noack T and Borger MA. Preoperative determination of artificial chordae length: Wishful thinking? *J Thorac Cardiovasc Surg.* 2017;154:1632–1633. [PubMed: 28890080]
28. Chawla SK, Shi W, McIver BV, Vinten-Johansen J, Frater RW and Padala M. Pre-clinical Experience with a Multi-Chordal Patch for Mitral Valve Repair. *Journal of cardiovascular translational research.* 2016;9:127–34. [PubMed: 26801477]
29. Chawla SK, Padala M, Chitwood WR Jr. and Frater RWM. Use of a New Expanded Polytetrafluoroethylene Multichordal Mitral Apparatus (MitraPatch) to Repair Complex Mitral Valve Lesions. *Innovations (Phila).* 2017;12:411–417. [PubMed: 29232298]
30. Padala M, Sacks MS, Liou SW, Balachandran K, He Z and Yoganathan AP. Mechanics of the mitral valve strut chordae insertion region. *J Biomech Eng.* 2010;132:081004. [PubMed: 20670053]

31. Fenoglio JJ, Jr., Tuan Duc P, Wit AL, Bassett AL and Wagner BM. Canine mitral complex. Ultrastructure and electromechanical properties. *Circulation research*. 1972;31:417–30. [PubMed: 5057021]
32. Oosthoek PW, Wenink AC, Wisse LJ and Gittenberger-de Groot AC. Development of the papillary muscles of the mitral valve: morphogenetic background of parachute-like asymmetric mitral valves and other mitral valve anomalies. *The Journal of thoracic and cardiovascular surgery*. 1998;116:36–46. [PubMed: 9671895]

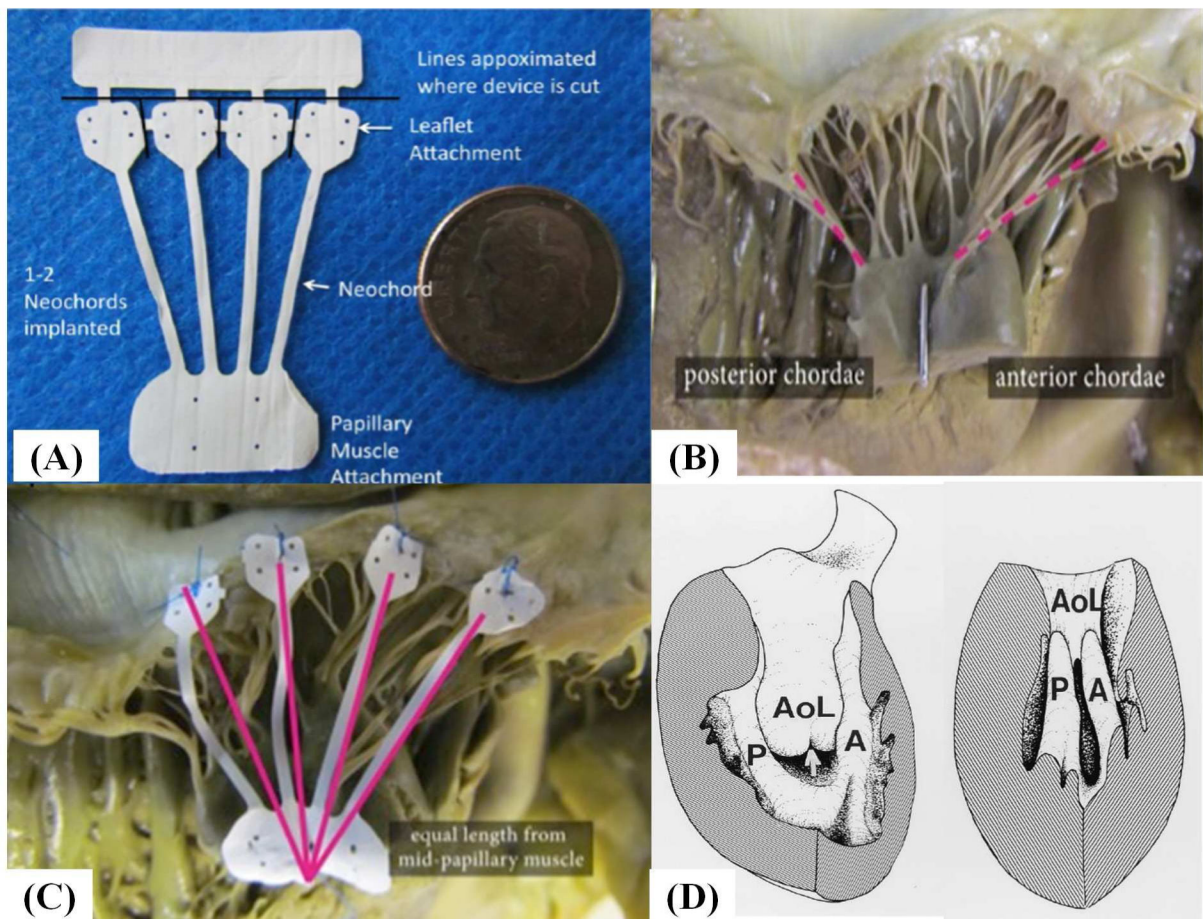


Figure 1:

(A) Photograph of the ePTFE multi-chordal mitral valve apparatus. The bottom part of the device is a single papillary muscle attachment section (neo papillary muscle), with four chordae emerging from it and each chord ending in a small leaflet section (neo leaflet). These neoleaflet are connected to each other, and can be separated by cutting the small connecting segments. The top most rectangular section enables attachment of the implant to a delivery handle; (B) Photograph of a cadaveric heart depicting unequal distances from the papillary muscle tip to the chordal insertions, but equal distances from the base of the papillary muscle to the chordal insertion; (C) The multi-chordal apparatus implanted on the mitral valve in the human heart; (D) Schematic reproduced from Oosthoek et al. about the developmental origins of the two papillary muscles in the human heart, forming the basis for equal lengths of chordae from the base to their insertion into the leaflets

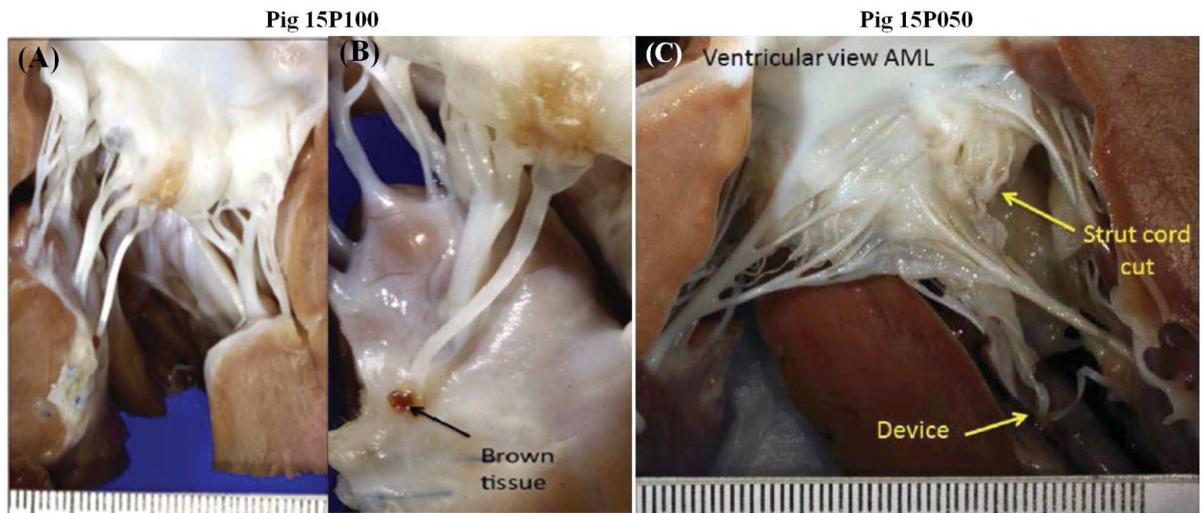


Figure 2:

(A) Device from pig 15P100, which is a representative image of the intact chordae observed in 5 of the 6 animals at 150–180 days after implantation (B) Photograph of the device from pig 15P050 in which it dehisced from the leaflet insertion site due to erroneous transection of the native strut chord along with marginal chordae prior to insertion;

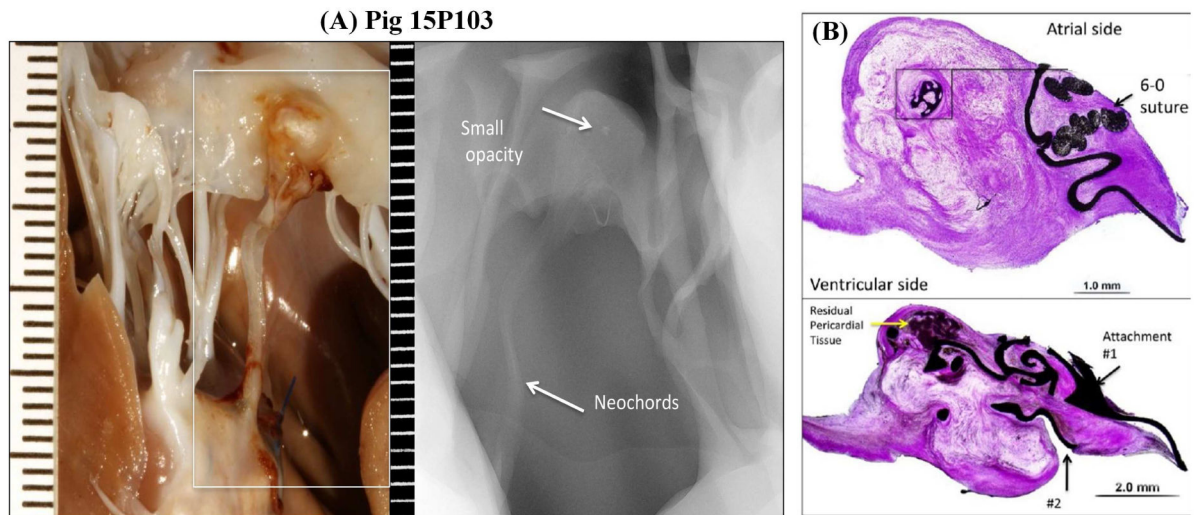


Figure 3:
 (A) Inset of the opaque region at the leaflet insertion site from pig 15P103, and a corresponding radiographic image depicting a small nodule (B) Histopathologic evaluation of the this site demonstrated metaplastic ossification in the pericardium pledget

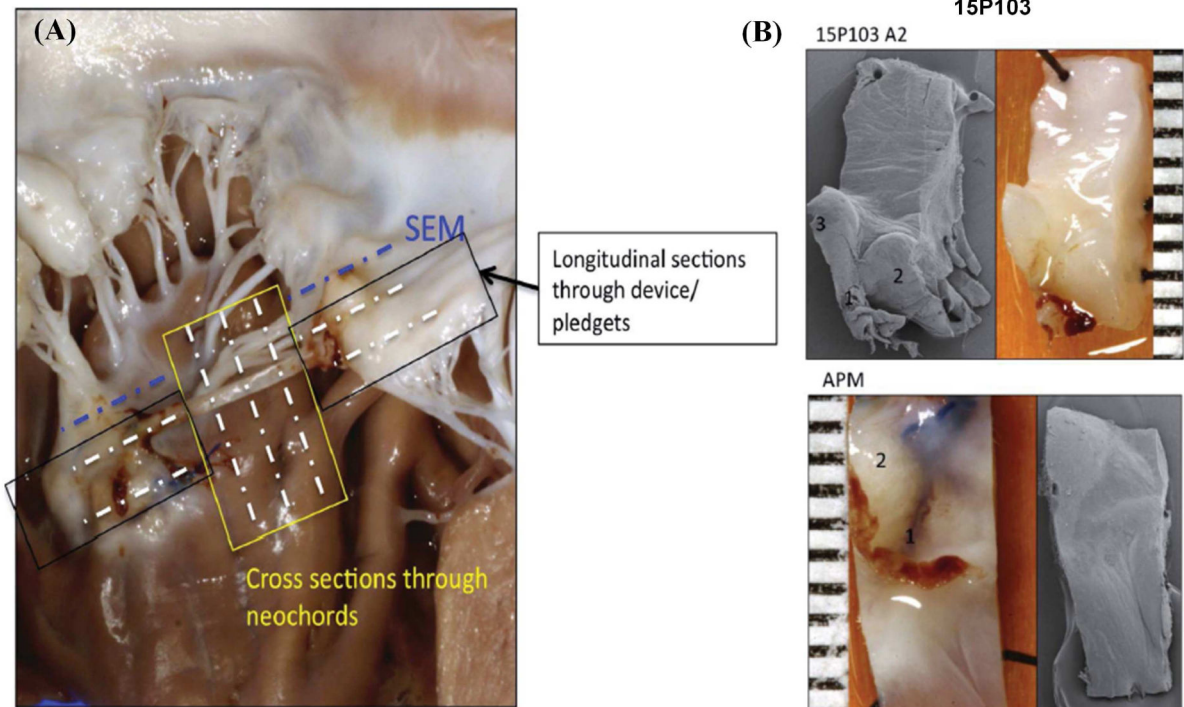


Figure 4:

(A) Schematic of the different cross sections obtained for histopathology and scanning electron microscopy from each sample; (B) Scanning electron microscopy of representative sections from a pig at the leaflet insertion and papillary muscle insertion, which do not depict any thrombus attachment, but demonstrate a small surface that is potentially endothelialized.

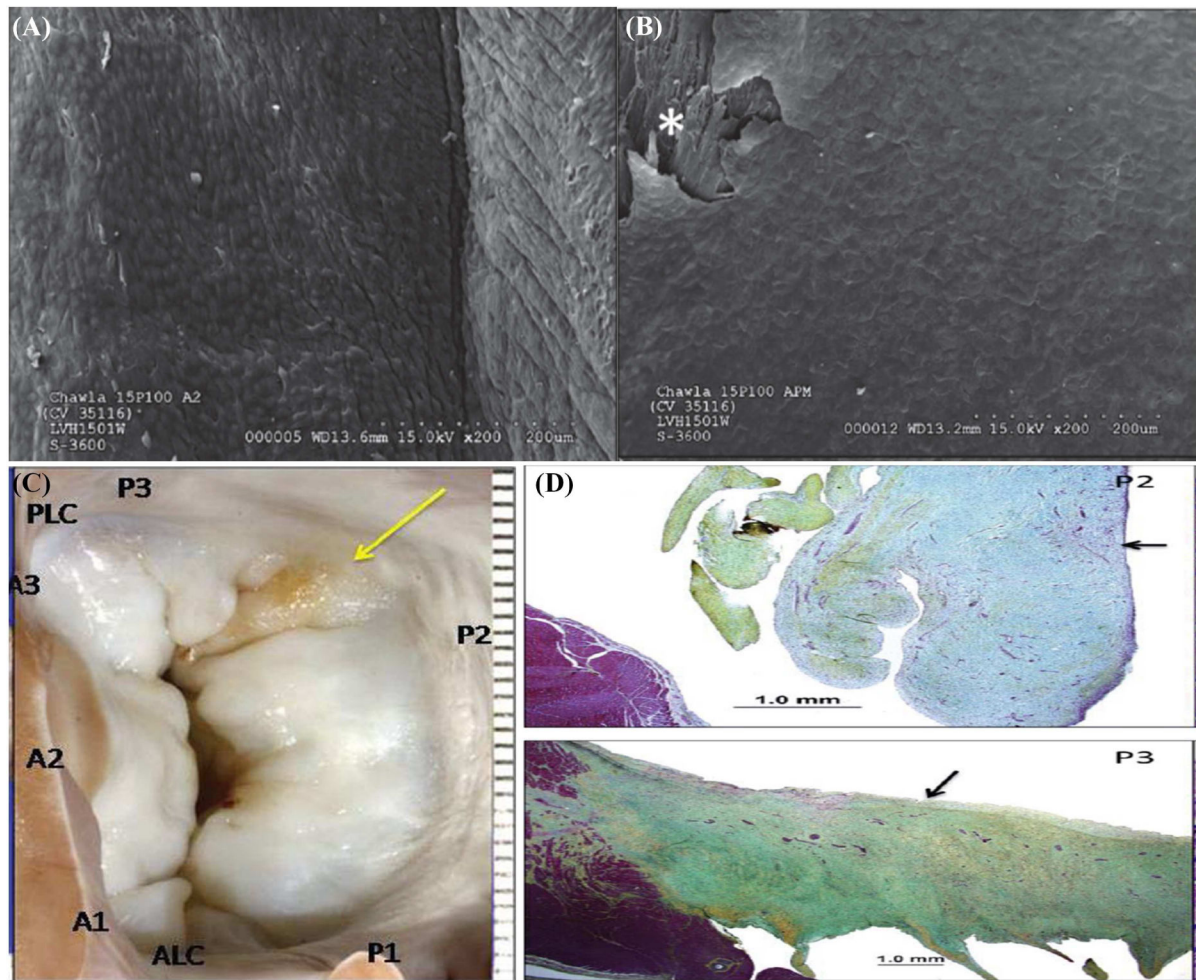


Figure 5:
 (A) High magnification scanning electron microscopy images of the leaflet attachment sites in pig 15P100 depicting complete endothelialization of the neoleaflet region; (B) Similar endothelialization of the papillary muscle attachment section in the same pig. (C) Atrial view of the mitral valve from pig 15P100, depicting slight yellow color of the posterior leaflet opposite to the device; (D) Movat's pentachrome staining depicted local thickening with focal hemosiderin deposits without any discrete injury to the leaflet that could be identified on these sections.

Summary of outcomes in the swine used in this study

Table 1:

S.No	Pig Number	Location of cut chordae	Number of cut chordae	Pre-repair MR	Number of neochoords	Leaflet Pledget material	Papillary pledget material	Post-repair MR	Follow-up time (days)	Explant findings
1	15P098	A1 & A2	3	Severe	2	Pericardium	PTFE	Grade 1	0	Intact device/no thrombus
2	15P050	A2 strut	1	Severe	1	Pericardium	PTFE	Grade 1	182	Strut chord was cut in error. Repair with neochoord required superior attachment, resulting in dehiscence
3	15P099	A2	2	Severe	1	Pericardium	PTFE	Grade 1	181	Intact device/well organized small thrombus at leaflet attachment site without systemic embolization
4	15P100	A2	1	Severe	1	PTFE	PTFE	Trace	152	Intact device/no thrombus
5	15P101	A2	1	Severe	1	PTFE	PTFE	None	151	Intact device/well organized small thrombus at leaflet attachment site without systemic embolization
6	15P103	A2	3	Severe	2	Pericardium	PTFE	Trace	153	Intact device/no thrombus
7	15P104	A2	3	Severe	2	PTFE	PTFE	None	152	Intact device/no thrombus

Species: *Sus scrofa* (porcine); **Breed:** Landrace cross; **Source:** Oak Hill genetics; **Age at Procedure:** 3.7 – 4.7 months; **Weight at procedure:** 54.3 – 60.6 kg; **Gender:** Female (nulliparous and non-pregnant); **Number of animals:** 7

Table 2:

Echocardiographic observations and findings from study animals

Animal Number	Observation Time Point	Regurgitation	Mitral Gradient (mmHg)			Mitral Valve Prolapse		Mitral Valve Flail	
			Peak	Mean	Anterior	Posterior	Anterior	Posterior	
Acute Pilot Animal									
15P098	Day 0 pre	3	NA	NA	Severe	Absent	Moderate	Absent	
	Day 0 post	1	NA	NA	Absent	Absent	Absent	Absent	
Chronic Animals									
15P050	Day 0 post	1	1.0	0.4	Absent	Absent	Absent	Absent	
	Day 6	2-3	3.7	1.5	Moderate	Absent	Mild	Absent	
	Day 28	2	2.6	1.3	Moderate	Absent	Absent	Absent	
	Day 56	2	2.3	1.1	Mild	NA	Absent	Absent	
	Day 93	2-3	4.3	1.6	Severe	Absent	Moderate	Absent	
	Day 154	3	12.4	4.9	Moderate	Absent	Mild	Absent	
	Day 182	3	3.2	1.4	Moderate	Absent	Absent	Absent	
15P100	Day 4	Trace	2.2	1.4	Absent	Absent	Absent	Absent	
	Day 26	0	2.8	1.3	Absent	Absent	Absent	Absent	
	Day 54	0.5	1.7	0.7	Absent	Absent	Absent	Absent	
	Day 91	0	2.1	0.8	Absent	Absent	Absent	Absent	
	Day 152	0	1.2	0.3	Absent	Absent	Absent	Absent	
	Day 3	0	2.4	1.6	Absent	Absent	Absent	Absent	
	Day 25	1-2	2.1	1.1	Mild	Absent	Absent	Absent	
15P101	Day 53	0	1.7	0.9	Absent	Absent	Absent	Absent	
	Day 90	0.5	1.1	0.5	Absent	Absent	Absent	Absent	
	Day 151	0.5	0.8	0.3	Absent	Absent	Absent	Absent	
	Day 5	1-2	3.9	2.0	Absent	Absent	Absent	Absent	
	Day 27	Trace	1.9	1.0	Absent	Absent	Absent	Absent	
	Day 55	0.5	1.7	0.8	Absent	Absent	Absent	Absent	
	Day 92	0	2.0	1.4	Absent	Absent	Absent	Absent	
15P103	Day 153	1	0.8	0.5	Absent	Absent	Absent	Absent	

Animal Number	Observation Time Point	Regurgitation	Mitral Gradient (mmHg)		Mitral Valve Prolapse		Mitral Valve Flail	
			Peak	Mean	Anterior	Posterior	Anterior	Posterior
15P104	Day 4	0.5	3.9	2.3	Absent	Absent	Absent	Absent
	Day 26	0.5-1	3.1	1.0	Absent	Absent	Absent	Absent
	Day 54	0.5	1.5	0.3	Absent	Absent	Absent	Absent
	Day 91	0.5	1.7	0.6	Absent	Absent	Absent	Absent
	Day 152	Trace	1.1	0.6	Absent	Absent	Absent	Absent
15P099	Day 5	1	7.9	4.0	Mild	Absent	Absent	Absent
	Day 27	0.5	2.0	0.6	Absent	Absent	Absent	Absent
	Day 55	1-2	1.8	0.7	Mild	Absent	Absent	Absent
	Day 92	1	2.2	0.7	Mild	Absent	Absent	Absent
	Day 153	1-2	3.1	1.6	Mild	Absent	Mild ⁴	Absent
	Day 181	1	1.3	0.7	Absent	Absent	Absent	Absent